Sixth International Conference on Durability of Concrete Structures
18 - 20 July 2018
University of Leeds, Leeds, West Yorkshire, LS2 9JT, United Kingdom

Paper Number PSE23

Load-bearing Capacity of Corroded Reinforced Concrete Structures Caused by Carbonation and Exposed to XC4

E. Sistonen

Aalto University, Department of Civil Engineering, Aalto, Finland

ABSTRACT

Concrete corrosion can be visualized as a combination of chemical reaction on concrete and electrochemical reaction on steel reinforcement. Failure of steel reinforcement due to corrosion can inflict significant stress on concrete during load distribution. As such, it is necessary to analyse the long-term effects of corrosion on the load bearing capacity and bending strength of steel reinforcement. This research investigated the mechanical and electrochemical properties of concrete exposed to long-term corrosion for a period of 16 years. Non-destructive testing like crack width measurements, visual examination, electrochemical measurements using Galva Pulse and determination of average chloride content were undertaken to identify the state of corrosion and to ascertain the impact of corrosion on the chemical properties of concrete. Further testing included mechanical tests for load-bearing capacity and compressive strength. The electrochemical measurement results signified the condition of the corroded beam specimens and provided the degree of corrosion at the time of experimentation. Beam specimens with large crack widths, and reinforcement bar diameters showed poor resistance to corrosion. Load-bearing capacities of above mentioned corroded beam specimens were lower when compared to the original measurements before exposure started. The reason was the reduction in cement-steel bonding due to the expansion of rust in the structure. However, compressive strength of concrete almost doubled due to continuous hydration occurring during the cyclic wetting and drying period. This increase in compressive strength of concrete compensated the reduction in load-bearing capacity.

Keywords: Load-bearing Capacity, Carbonation, Corrosion, Reinforcement.

1.0 INTRODUCTION

The phenomenon of corrosion in concrete has been extensively studied using experimental techniques and numerical modelling methods. Early detection of corrosion can help save maintenance costs and extend the durability of structures considerably. The residual load-bearing capacity of corroded beams is dependent on the extent of loss of steel cross section due to the presence of corrosion. Corrosion also results in loss of concrete cover and causes spalling at the edges of the structure. Since the reduced load-bearing capacity is detrimental to the serviceability of a structure, corrosion has to be dealt with accordingly. The role of the reinforcement bar material in a deteriorated reinforced concrete structure focuses on the strength of the structure. Thus, the load-bearing capacity of the structure depends mostly on the loss of bar section. In that case the research problem focuses on methods that ensure the functioning of the structure in its fulfilled service and ultimate limit state in the long term.

The aim of this study is to determine the effects of corrosion on the load-bearing characteristics of concrete. It included several objectives like calculation of concrete crack widths, and electrochemical measurements of concrete samples exposed to corrosion for a 16 years period. Research methods included literature studies and laboratory experiments. Studied parameters included crack width, electrochemical variables like potential, current and resistivity of the concrete specimens. Visual inspection of the beam specimens was also undertaken along with these tests. Later, load-bearing capacity tests were performed in order to compute the load and moment values and then those values were compared to that of the beam specimens before the exposure started. The research was mainly concentrated on the electrochemical parameters, crack width and the load-deflection values for all types of beam specimens. In addition, moisture-temperature variations, carbonation depth and average chloride content were also recorded. The exposure class under consideration was XC4 i.e. corrosion caused by carbonation in a cyclic wet and dry condition.

2.0 EFFECT OF CORROSION ON LOAD-BEARING CAPACITY

The reduction in load-bearing capacity of reinforced concrete structures can be attributed to the loss of cross-sectional area of the rebars caused due to

their localized corrosion (Dang *et al.*, 2016). The reduction in load-bearing capacity can be attributed to the loss of cross-sectional area of the rebars caused due to their localized corrosion (Dang *et al.*, 2016). According to the pull-out tests and beam tests (Wei-liang and Yu-xi, 2000), the bond strength of plain steel bars and concrete initially increases with increase in corrosion, but then declines. The deflection point depends on the cracking of concrete cover. After the initial increase of the bond strength, it gradually decreases after a certain point and thereafter the cracking of concrete cover seems to have negligent effect on the bonding strength of concrete. Tensile strength of corroded cylinder specimens after seven years of exposure were studied (Sistonen, 2009). The most corroded areas were often located between cracks or in the upper or lower part of the cylinder specimens. The location did not correlate with crack width. According to the results of the tensile tests, the mechanical properties of reinforcements that were taken from cylinder specimens after seven years of exposure did not fulfil the standard requirements. Concrete with w/c ratio 0.70 was used.

3.0 EXPERIMENTAL SET-UP

Four types of reinforcement bars were used; ordinary steel, hot-dip galvanised steel, weathering steel (TENCOR), and austenitic stainless steel (grade AISI 304). A detailed description of the reinforcement bars used is given in Table 1.

A total of 243 beams with dimensions of 100x80x700 to 100x100x815 mm (Table 1) were cast. Two of the beam specimens were unreinforced. The Rapid hardening cement type CEM II/A-LL 42.5 R produced by Finnsementti Oy (Ltd.) was used to produce the test specimens. The modified naphthalene formaldehyde poly-condensate based superplasticiser YLEIS-PARMIX® was used. The aggregates were mainly granite. Concrete with water to cement ratio 0.46 was used. The amount of cement was 428 kg/m^3. Concrete cover for all the reinforcement bars was 5 mm. As a result of the geometry, the maximum aggregate size was limited to 8 mm for the beam specimens. The amount of aggregates was 1610 kg/m^3. Air-entrained concrete was used to produce the beam specimens. The amount of superplasticiser was 5.1 kg/m^3. The concrete for the beam specimens was ordered from Lohja Rudus Oy (Ltd.).

Protective pore ratio of the hardened concrete for the beam specimens were measured with six samples according to standard (SFS 4475, 1988). Mean value for protective pore ratio p_r was equal to 0.30 and standard deviation was 0.01. The result fulfilled the old requirements for exposure class E3b (difficult circumstances, chloride attack, and freezing and thawing stress) which were 0.25 (By 32, 1992). After curing, artificial cracks were made in the concrete specimens. The cracks in the beam specimens were made by three-point bending so that the bars yielded with different loads (Fig. 1 and Fig. 2).

Table 1. Reinforcement bar types

| Code	Reinforcement bar type	Type of beam	Reinforcement bar diameter, Ø (mm)	Beam dimensions, b×h×l (mm^3)
A500HW/ Ø8	Weldable hot-rolled ribbed steel bar	A8	8	100×80×700
A500HW/ Ø8/ZN	Weldable hot-rolled ribbed steel bar, hot-dip galvanised	A8-Zn	8	100×80×700
B500K/ Ø8	Cold-worked ribbed steel bar	B8	8	100×80×700
B500K/ Ø8/ZN	Cold-worked ribbed steel bar, hot-dip galvanised	B8-Zn	8	100×80×700
B500K/ Ø7	Cold-worked ribbed steel bar	B7	7	100×80×700
B600KX/ Ø7	Austenitic stainless ribbed steel bar	B7-RST	7	100×80×700
A500HW/ Ø12	Weldable hot-rolled ribbed steel bar	A12	12	100×100×800
TENCOR/ Ø12	Weathering ribbed steel bar	C12	12	100×100×815
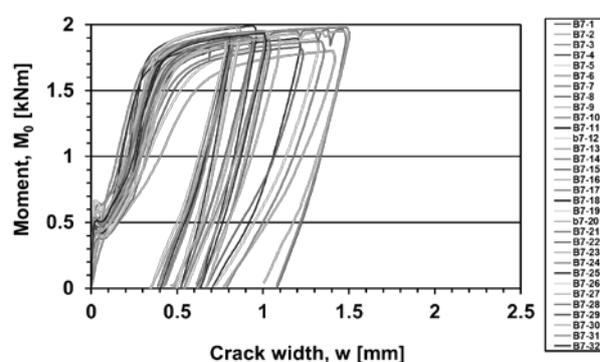
Fig. 1. Example of making cracking of beams before durability tests: cold-worked ribbed steel bar (B7)
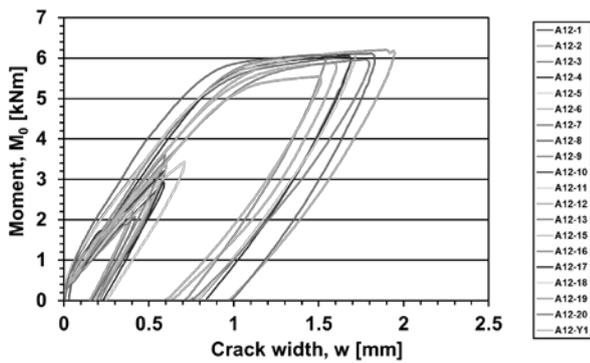
Fig. 2. Example of making cracking of beams before durability tests: weldable hot-rolled ribbed steel bar (A12)

The cracks were mainly situated in the middle of the beam specimens. After that beam specimens were exposed to accelerated carbonation for achieving neutralization of concrete. The beam specimens in the durability tests were carbonated deeply enough to achieve an active state of corrosion.

Approximately half of the beam specimens were exposed to tap water. The wetting and drying cycles of the beam specimens with the tap water simulated the exposure class XC1 for the first seven years. After that, the cycling was changed so that the exposure class was XC4 until the end of the durability tests. The studies included the determination of the carbonation depth and average chloride content, concrete compressive strength, thin section analysis, spacing factor analysis, and the measurement of the pH values, electrochemical properties, crack width, and moisture condition. Furthermore, optical microscopy and ESEM (environmental scanning electron microscope) studies were performed. After the durability test load-bearing capacity test was performed by three-point bending (Fig. 3). Each measurement in the durability tests was needed in the study to analyse the long-term properties of reinforcement bars.

4.0 TEST RESULTS

The carbonation depth of the beam specimens in uncracked concrete, and also in cracked concrete longitudinally to the reinforcement bars, increased by approximately two millimetres during the wetting and drying exposure. Average chloride content of tap water was 0.05 wt% Cl^-. Crystallisation by ettringite was not noticed in the microscopic cracks. To judge from the pore structure and the results of the spacing factor analysis, the concrete samples were not frost-resistant in moisture loading. According to the determined pH values of the tap water of the beam specimens, the OH^- ions dissolved in the tap water. The results show the leaching of some alkalis into the solution. That is seen in the increase of the pH values of the tap water of the beam specimens as a function of time.

The electrochemical measurements of the beam specimens were performed after approximately six months, five years, and 15.8 years of exposure. The rates of corrosion were calculated according to the corrosion current values and are shown in Fig. 4.

Fig. 3. Example of load-bearing capacity test by three-point bending: weldable hot-rolled ribbed steel bar, hot-dip galvanised (A8Zn-13), failure by shear
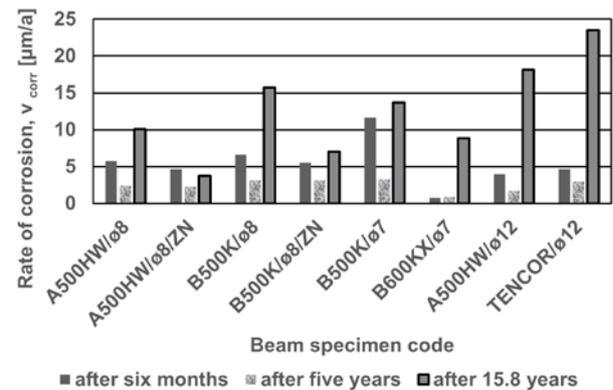

Fig. 4. Rate of corrosion of the beam specimens exposed to tap water

The crack widths of the beam specimens were measured in the context of the electrochemical measurements. Measured crack width values are shown in Fig. 5.
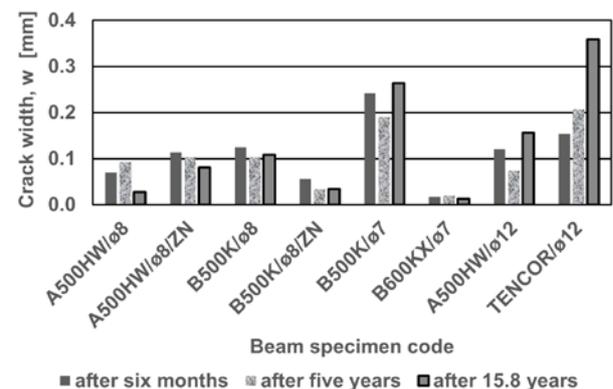

Fig. 5. Crack width of the beam specimens exposed to tap water

Load-bearing tests were performed on all beam specimens exposed to tap water. These were done in order to accurately determine the effect of corrosion on the developed cracks and the extent of cracking developed further due to corrosion. Examples of crack width-moment curves after 16 years of exposure are presented in Fig. 6, and Fig. 7. These examples are comparable to Fig. 1 and, Fig. 2, respectively.
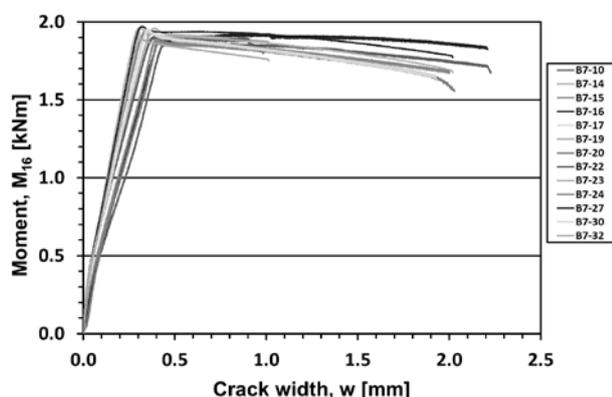

Fig. 6. Example of load-bearing test result of beams after durability tests: cold-worked ribbed steel bar (B7), failure by bending
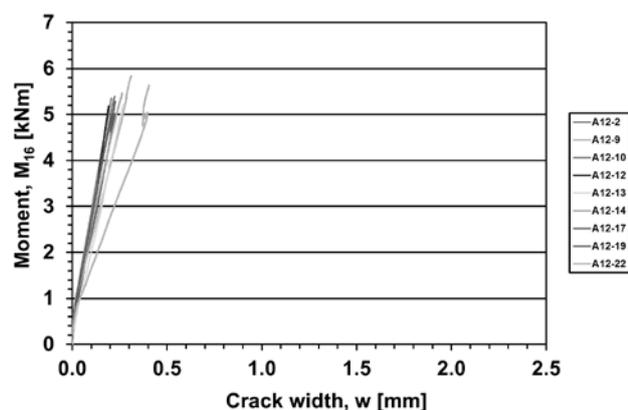

Fig. 7. Example of load-bearing test result of beams after durability tests: weldable hot-rolled ribbed steel bar (A12), failure by shear

Load-bearing capacity test result of beam specimens before and after the durability tests are presented in Table 2, and Table 3. Only comparable test results were used.

The cubic compressive strength of concrete was 47.3 MPa, 28 days after the casting, and 85.3 MPa after 16 years of exposure to wetting and drying cycles in tap water, respectively. Compressive strength was performed on the beam specimen that was unreinforced and exposed to 10 % of sodium chlorides in a cyclic wet and dry condition for 16 years. That factor was accounted for the test result.

Table 2. Load-bearing test result of beams before durability tests

Type of beam	Number of beams, n_0 (-)	Mean value of moment, M_0 (kNm)	Standard deviation, σ_0 (kNm)	Coefficient of variation, v_0 (-)
A8	8	2.09	0.04	0.02
A8-Zn	9	2.02	0.22	0.11
B8	8	2.24	0.06	0.03
B8-Zn	9	1.92	0.06	0.03
B7	32	1.91	0.05	0.02
B7-RST	10	1.97	0.16	0.08
A12	9	6.01	0.19	0.03
C12	26	5.23	0.51	0.10
Sum.	111			

Table 3. Load-bearing test result of beams after 16 years of exposure of durability tests

Type of beam	Number of beams, n_{16} (-)	Mean value of moment, M_{16} (kNm)	Standard deviation, σ_{16} (kNm)	Coefficient of variation, v_{16} (-)	Ratio of moments, M_{16}/M_0 (-)
A8	12	2.21	0.09	0.04	1.06
A8-Zn	10	2.22	0.06	0.03	1.10
B8	13	2.23	0.06	0.02	0.99
B8-Zn	12	2.24	0.04	0.02	1.17
B7	14	1.92	0.04	0.02	1.01
B7-RST	11	2.15	0.16	0.08	1.09
A12	9	5.29	0.29	0.06	0.88
C12	9	4.02	1.07	0.27	0.77
Sum.	90				

5.0 ANALYSIS OF THE TEST RESULTS

The hot-dip galvanised steel showed a lower rate of corrosion in comparison with ordinary steel. The comparison of the measured crack width and rate of corrosion values generally showed no correlation independently of the exposure duration. However, beam specimen types A12 and C12 showed strong correlation between increased crack width and rate of corrosion as a function of time. The rate of corrosion was found to be the highest in the case of weathering steel (type C12) in tap water beam specimens.

State of corrosion based on $E_{corr} - \log i_{corr}$, $E_{corr} - R$, and $\log i_{corr} - R$ graphs of reinforcement bars for the beam specimens exposed to tap water after 15.8 years of exposure showed the following: moderate corrosion risk for ordinary and weathering reinforcement bars, low risk of corrosion for hot-dip

galvanised and austenitic stainless reinforcement bars.

Failure mechanisms of beams based on load-bearing tests is presented in Table 4. Bending was realised in 62 % of beams tested, and shear failure in 38 %, respectively. Totally, 22 % with dimension 12 mm bars (types A12 and C12) were also failure by anchorage (Fig. 8). That was strongly affected by the recognised longitudinal cracking that also influenced on transversal crack width and rate of corrosion values.

Based on the statistical analysis, weathering steel bar showed large variation. The logical explanation for this is the severe corrosion and longitudinal cracking, among others.

Table 4. Failure mechanisms of beams based on load-bearing tests

Type of beam	Number of beams, n_{16} (-)	Bending	Shear	Longitudinal cracking	Remark
A8	12	12		5	
A8-Zn	10	7	3		
B8	13	11	2		
B8-Zn	12	12			
B7	14	14		1	One bar broke off after failure
B7-RST	11		11		
A12	9		9	9	Also anchorage failure in two beams
C12	9		9	7	Also anchorage failure in two beams
Sum.	90	56	34	22	

Example of longitudinal cracking of severe corroded beam after load-bearing capacity test by three-point bending is presented in Fig. 9. As a logical result, that cracking is concentrated on types A12 and C12 beams that produce more spalling forces to the concrete cover. In addition, hot-dip galvanised beams did not cause longitudinal cracking. The main corrosion product of zinc, zinc oxide (ZnO), occupies 1.5 times the volume of the original zinc (Yeomans, 2004; Porter, 1991). However, the volume of zinc oxide is approximately 1/3 less (Yeomans, 1993) than the volume of the corrosion products of ordinary steel. Corrosion products are friable, loose, and powdery minerals. The products are able to migrate away from the bar and into the adjacent porous concrete matrix, where they fill small voids and micro-cracks (Hoke *et al.*, 1981; Yeomans, 1993). In that case the local tensile stresses in the concrete are also lower and zinc corrosion products do not exactly cause the concrete cover to deteriorate. That was realised afterwards with opened beams (Fig. 10).

One bar broke off after failure. That beam (type B7) should be studied closely afterwards to conclude the reason for this. Maybe, the localised (pitting) corrosion has influence on that.

Fig. 8. Example of severe corroded beam after load-bearing capacity test by three-point bending: weldable hot-rolled ribbed steel bar (A12-22), failure by shear and anchorage

Fig. 9. Example of longitudinal cracking of severe corroded beam after load-bearing capacity test by three-point bending: weldable hot-rolled ribbed steel bar (A12-17), failure by shear

Fig. 10. Example of the opened beam specimen after load-bearing capacity test by three-point bending: cold-worked ribbed steel bar, hot-dip galvanised (B8Zn-29), failure by bending. Localised corrosion spots for instance at the crack (crack width w = 0.18 mm)

Clogging of cracks for beam specimens exposed to tap water after six months, five years, and 15.8 years of exposure is presented in Table 5. It can be seen that the alkalis and corrosion products have very effectively formed barrier against harmful

substances. That may have had effect on the decreased rate of corrosion due to lack of oxygen.

Table 5. Clogging of cracks for beam specimens exposed to tap water after six months, five years, and 15.8 years of exposure

Class	Six months of exposure	Five years of exposure	15.8 years of exposure
0 = no visible crack	7	5	25
1 = crack partly settled	12	28	18
2 = crack settled	6	2	41
3 = crack not settled	56	46	6
Sum.	81	81	90

6.0 DISCUSSION

Factors influencing the results of the electrochemical measurements are the corrosion products which form on the surfaces of the reinforcement bar or environmental conditions, such as moisture content and temperature (Andrade, 2000). On the basis of the measurement results it can be concluded that there was a local anodic area in the reinforcement bar at the crack which was surrounded by a large cathodic area extending away from the crack into the sound concrete. This means that even in a high-quality concrete cracking has significance for the durability of the reinforcement bar materials by reducing macro-level corrosion. This is understandable because with a high water-to-binder ratio anodic areas may spread near the crack into the uncracked area. In that case micro-level corrosion currents also increased in widespread anodic areas. The water-to-binder ratio has a significant influence on the formation of macro-level corrosion, and the values of macro- and micro-level corrosion (Mohammed *et al.*, 2003; Otsuki *et al.*, 2000). Furthermore, localised corrosion with a low water-to-binder ratio may lead to the passivation of the steel as a result of the settlement of the crack by corrosion products and alkalis (Fig. 11).

There are a number of sources of errors related to the electrochemical measurements. One of the major problems is non-uniform corrosion along the reinforcement bar, while the results obtained represent an average rate of corrosion. Consequently, local severe corrosion is not detected. Furthermore, the values obtained are not absolute and can be used for comparison between the beam specimens. Another issue is the effect of the cracks on the measured values. It is commonly accepted (Andrade, 2004) that with a larger crack width the corrosion current and rate of corrosion should increase, while the corrosion potential and resistivity of the concrete should decrease. This tendency was not found in the present studies. In the author's opinion it could be related to varying crack widths and the occasional clogging of the cracks with leaching products.
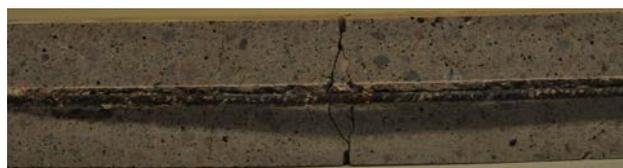

Fig. 11. Example of the opened beam specimen after load-bearing capacity test by three-point bending: cold-worked ribbed steel bar (B7-19), failure by bending. Longitudinal cracking observed. Localised corrosion spots for instance at the crack (crack width w = 0.22 mm)

The reinforcement bars were already loaded to their yield limit before the corrosion tests and the testing arrangements differ from the stresses found in the service limit state, which have a secondary effect on the usability of the results of the load-bearing capacity, electrochemical and crack width measurements. Furthermore, it should be noted that the structure may also crack as a result of imposed deformations (Nagy, 1997).

The beam specimens were not fully comparable because the failure mechanisms were different. Thus, the bending moment of the shear failure is not scientifically exact but it can be accepted in this kind of comparisons between exposed and unexposed beam specimens. Those unexposed beam specimens that were not yielded, were also excluded from analyses. It should also be noted that for some unexposed beam specimens external stirrups (especially types A12 and C12) were used to enable larger crack width values, and to avoid shear failure.

The crack width do not necessary correlate with the load-bearing values. The observed longitudinal cracking is more dominant that the transvers cracking in the case of the beam specimens. Furthermore, the corrosion of the anchorage area effect on the shear failure. In addition, the clogging of the cracks has an influence on the durability. Above-mentioned factors decrease the effect of the crack width on the load-bearing capacity of the beam specimens.

The long-term hydration process of the cement matrix compensated the decrease of the load-bearing capacity of the beam specimens. The compressive strength of concrete after the durability test was approximately 80 % greater than one month after the casting. Huge amount of cracks were settled with the corrosion products and alkalis. Certainly, that influenced on the hydration process. The re-alkalization was not noticed: average value of the carbonation depth of the beam specimens after 15.8 years of exposure increased approximately couple of millimetres.

7.0 CONCLUSIONS

Corrosion effect on the load-bearing capacity of the beam specimens but the increased compressive strength of concrete and the self-healing effect compensate that decrease. Hot-dip galvanised and austenitic stainless steel reinforcement bars increased the load-bearing capacity of the beam specimens. In the case of ordinary reinforcement steels with the bar diameter of seven and eight millimetres, the load-bearing capacity of the beam specimens whether was the same or slightly increased compared to the unexposed situation. That is logically explained with lower spalling stress to the concrete cover. In the case of ordinary and weather reinforcement steels with the bar diameter of 12 mm, the load-bearing capacity of the beam specimens decreased compared to the unexposed situation. The logical explanation is the greater spalling stress to the concrete cover.

The correlations between crack width and corrosion rate were made on the same type of beam specimens. The comparison of the measured crack width of concrete with the rate of corrosion values showed no correlation independent of the exposure duration. There was a local anodic area on the reinforcement bar at a crack which was surrounded by a large cathodic area extending away from the crack into the sound concrete. This means that in high-quality concrete cracking has significance for the durability of the reinforcement bar materials.

Further research needed after the load-bearing tests is the micro level studies of the corroded beam specimens to identify the interfacial transition zone between the cement matrix and the different steel bar types. Furthermore, the load-bearing capacity of the chloride-contaminated beam specimens exposed to corrosion due to 10 % of sodium chlorides in a cyclic wet and dry condition (XD3) should be made to compare with the test results that were analysed in this study.

Acknowledgement

References

Andrade, C., Gulikers J., Polder, R., Vennesland, Ø., Elsener, B., Weider, R., Raupach, M. (2000). Recommendations of RILEM TC-154-EMC: "Electrochemical Techniques for measuring Metallic Corrosion" Test Methods for On-site Measurement of Resistivity of Concrete. Materials and Structures, Vol. 33, No. 234, pp. 603-611.

By 32 (1992). Durability Guideline and Service Life Dimensioning of Concrete Structures, Concrete Association of Finland, 1992. (in Finnish).

Dang, V.H., François, R., Coronelli, D. (2016). Shear behaviour and load capacity of short reinforced concrete beams exposed to chloride environment. European Journal of Environmental and Civil Engineering, 20(4), pp.379–395. Available at: http://dx.doi.org/10.1080/19648189.2015.1036129.

Hoke, J.H., Pickering, H.W., Rosengarth, K. (1981). Cracking of Reinforced Concrete. ILZRO Project ZE-271. International Lead Zinc Research Organisation, Research Triangle Park, NC, USA.

Mohammed, T., Otsuki, N., Hamada, H. (2003). Corrosion of Steel Bars in Cracked Concrete, Journal of Materials in Civil Engineering, Vol. 15, No. 5, pp. 460-469.

Nagy, A. (1997). Cracking in Reinforced Concrete Structures Due to Imposed Deformations, (Doctoral thesis) Lund Institute of Technology, Rapport TVBK-1012. Lund, Sweden, 90 p. ISSN 0349-4969.

Otsuki, N., Miyazato, S., Diola, N., Suzuki, H. (2000). Influences of Bending Crack and Water-Cement Ratio on Chloride-Induced Corrosion of Main Reinforcing Bars and Stirrups, ACI Materials Journal, Vol. 97, No. 4, pp. 454-464.

Porter, F. (1991). Zinc Handbook, Properties, Processing, and Use in Design. New York, USA: Marcel Dekker, Inc. 629 p. ISBN 0-8247-8340-9.

SFS 4475 (1988). Concrete. Frost resistance. Protective pore ratio. Finnish Standards Association SFS, 2 p. (in Finnish).

Sistonen, E. (2009) Service life of hot-dip galvanised reinforcement bars in carbonated and chloride-contaminated concrete. TKK structural engineering and building technology dissertations. 161 p. + app. 16 p. Available at: http://urn.fi/URN:ISBN:978-952-248-168-9.

Sreekala, S. (2017). Load bearing capacity of corroded reinforced steel bars. Master's Thesis. Aalto University. 42 p. + app. 63 p.

Wei-liang, J., Yu-xi, Z. (2001). Effect of corrosion on bond behaviour and bending strength of reinforced concrete beams. Journal of Zhejiang University-SCIENCE A, 2(3), pp.298–308. Available at: https://link.springer.com/article/10.1007/BF02839464.

Yeomans, S.R. (1993). Coated Steel Reinforcement in Concrete Part 1. Corrosion Management, Vol. 2, No. 4, pp. 18-29.

Yeomans, S.R. (2004). Galvanized Steel in Reinforced Concrete, Elsevier B.V., Amsterdam, The Netherlands, 297 p. ISBN 0-08-044511-X.